11th Australasian Fluid Mechanics Conference
University of Tasmania, Hobart, Australia
14-18 December 1992

LOW REYNOLDS NUMBER EFFECTS ON NEAR-WALL TURBULENCE

R.A. ANTONIA[1] and J. KIM[2]

[1]Department of Mechanical Engineering, University of Newcastle, NSW 2308, AUSTRALIA

[2]Center for Turbulence Research, NASA-Ames Research Center, Moffett Field, CA 94035, USA

ABSTRACT

Direct numerical simulations of a fully developed turbulent duct flow for two relatively small values of the Reynolds number ($h^+ = hU_\tau/\nu = 180$ and 395, where h is the duct half-width, U_τ is the friction velocity, ν is the kinematic viscosity of the fluid) are used to examine the influence of h^+ on various turbulence quantities in the near-wall region ($y^+ \lesssim 40$). The limiting wall behaviour of various turbulence statistics indicates important increases in the rms value of the wall pressure and the streamwise vorticity and in the average energy dissipation and the Reynolds shear stress. The increases seem consistent with an increased stretching of streamwise vortices in the near-wall region.

INTRODUCTION

The limiting behaviour of turbulence near a wall is important from a modeling viewpoint. Compliance with this behaviour is necessary if turbulence models are to yield correct results near a wall (e.g. So et al., 1991a).

Direct numerical simulations (DNS) of turbulent flows have had a major impact on near-wall modeling (e.g. Mansour et al., 1989; Mansour, 1991) since they have provided estimates for terms in transport equations of the quantities that are usually modelled (e.g. the turbulent energy $\overline{q^2} \equiv \overline{u^2} + \overline{v^2} + \overline{w^2}$, or its individual components or the average turbulent energy dissipation ϵ). Many of these terms have not been accessible by measurement. The success of the use of DNS data bases in connection with near-wall modeling can be gauged from the improved calculation of ϵ in the near-wall region (e.g. So et al., 1991b).

One limitation of the present DNS data bases relates to the low Reynolds numbers at which they have been obtained so that extrapolation of the results to high Reynolds numbers should be done with caution. To date, near-wall turbulence models have not formally taken into account the likely dependence of the modelled transport equations on the Reynolds number. The DNS data bases for both the boundary layer (Spalart, 1988) and the channel flow (Kim et al., 1987; Kim, 1989) have been obtained at sufficiently different values of the Reynolds number to allow some insight into low Reynolds number effects. The present paper focuses mainly on the limiting wall behaviour in a channel flow and its dependence on the Reynolds number. Details of the simulations can be found in Kim et al. (1987), Kim (1989) and Antonia et al. (1991). A non-uniform mesh spacing was used in the y direction with a minimum spacing $\Delta y^+ \simeq 0.05$ at the wall (at both h^+ values).

ASYMPTOTIC NEAR-WALL BEHAVIOUR OF VARIOUS TURBULENCE QUANTITIES

Taylor series expansions of velocity and pressure fluctuations about their wall values have been written by a number of authors e.g. Townsend, 1956; Monin and Yaglom, 1971; Hanjalic and Launder, 1976; Chapman and Kuhn, 1986; Mansour et al., 1988). The expansions near $y = 0$ for u, v, w and p are re-written below (up to order y^{+3})

$$u^+ = b_1 y^+ + c_1 {y^+}^2 + d_1 {y^+}^3 \quad (1)$$

$$v^+ = c_2 {y^+}^2 + d_2 {y^+}^3 \quad (2)$$

$$w^+ = b_3 y^+ + c_3 {y^+}^2 + d_3 {y^+}^3 \quad (3)$$

$$p^+ = a_p + b_p y^+ + c_p {y^+}^2 + d_p {y^+}^3 \quad (4)$$

where the coefficients are functions of x^+, z^+ and t^+. The continuity equation and the momentum equations allow a few relations between these coefficients to be written (e.g. Mansour et al., 1988)

$$2c_2 = -(b_{1,1} + b_{3,3}) \quad (5)$$

$$a_{p,1} = 2c_1 \quad (6)$$

$$a_{p,3} = 2c_3 \quad (7)$$

$$b_{p,3} = 2c_2 \quad (8)$$

where $b_{1,1} \equiv \partial b_1/\partial x$, $b_{3,3} = \partial b_3/\partial z$ etc.

Expressions for several turbulence quantities can be derived from Eqs. (1) to (4). For example, the components of the vorticity fluctuation vector are given by (to order y^2)

$$\omega_x^+ \equiv w_{,2}^+ - v_{,3}^+ = b_3 + 2c_3 y^+ + (3d_3 - c_{2,3}){y^+}^2 \quad (9)$$

$$\omega_y^+ \equiv u_{,3}^+ - w_{,1}^+ = (b_{1,3} - b_{3,1})y^+ \quad (10)$$

$$\omega_z^+ \equiv v_{,1}^+ - u_{,2}^+ = -b_1 - 2c_1 y^+ + (c_{2,1} - 3d_1){y^+}^2 \quad (11)$$

There is no ${y^+}^2$ term in Eq. (10) since $(c_{1,3} - c_{3,1})$ is zero as a result of conditions (6) and (7). The product u^+v^+ is given by (to order y^3)

$$u^+v^+ = b_1 c_2 y^{+3} \quad . \tag{12}$$

The rms values of the coefficients of the first terms in Eqs. (1) to (4) and (9) to (11) are shown in Table I, where $(..)' \equiv \overline{(..)^2}^{\frac{1}{2}}$. Also shown are the average value values of the coefficient in Eq. (12) as well as the average values of the coefficients of the first terms in the expansions for the rms turbulent energy ($\overline{q^2} = \overline{u^2} + \overline{v^2} + \overline{w^2}$) and the average turbulent energy dissipation ϵ.

Table I : Effect of Reynolds Number on the RMS Values of Various Turbulence Statistics at the Wall

Quantity	$h^+ = 180$	$h^+ = 395$	Percentage Increase
u'^+/y^+	0.356	0.395	11
v'^+/y^{+2}	8.5×10^{-3}	1.1×10^{-2}	29
w'^+/y^+	0.190	0.245	29
q'^+/y^+	0.406	0.468	15
$-\overline{u^+v^+}/y^{+3}$	7.0×10^{-4}	9.5×10^{-4}	36
ϵ^+	0.164	0.219	34
p'^+	1.455	2.061	42
$(\partial p/\partial x)'^+$	4.767×10^{-2}	6.405×10^{-2}	34
$(\partial p/\partial y)'^+$	1.697×10^{-2}	2.297×10^{-2}	35
$(\partial p/\partial z)'^+$	6.926×10^{-2}	9.1×10^{-2}	31
$\omega_x'^+$	0.186	0.245	32
$\omega_y'^+/y^+$	2.7×10^{-2}	2.85×10^{-2}	6
$\omega_z'^+$	0.348	0.399	15

(Note that the limiting wall values of u'^+/y^+ and $\omega_z'^+$ should be the same as should those of w'^+/y^+ and $\omega_x'^+$).

The increase in u'^+/y^+ ($\equiv \overline{b_1^2}^{\frac{1}{2}}$) with h^+ is smaller than that in either v'^+/y^{+2} or w'^+/y^+. The increase in q'^+/y^+, which is dominated by the contribution from $\overline{u^2}$, is comparable to that in u'^+/y^+. The wall value of $\omega_z'^+$ should be identical to that of u'^+/y^+ [cf. the first terms on the right sides of Eqs. (1) and (11)]. Similarly, the wall value of ω_x' should be identical to that of ω'^+/y^+ [cf. the first terms on the right sides of Eqs. (3) and (9)]. Note that the increase in $-\overline{u^+v^+}/y^{+3}$ is much larger than that for any of the normal Reynolds stresses.

Other quantities in Table I which show important Reynolds number variations include the rms value of p and its derivatives, the average dissipation rate ϵ and the rms streamwise vorticity ω_x. Note that the rms value of $\partial p/\partial y$ is approximately twice as large as that for v/y^2, in reasonable agreement with the Neumann boundary condition at the wall, i.e. Eq. (8). It should also be noted that the Reynolds number variations exhibited by Table I is not unique to this flow; similar variations may be observed in Spalart's (1988) direct numerical simulation data for the boundary layer (e.g. p'^+ increases by about 42% between $R_\theta = 300$ and $R_\theta = 1410$, where R_θ is based on the free stream velocity and momentum thickness of the layer).

Note that the limiting wall value of $\omega_y'^+/y^+$ is practically unchanged, reflecting the apparent insensitivity of ω_y on the Reynolds number. It is also of interest to note that several quantities, which may be expressed as ratios of those shown in Table I, are essentially unaffected by the increase in h^+. For example, the limiting wall value of the structure parameter $(-\overline{u^+v^+}/y^+\overline{q^{+2}})$ is about 43×10^{-4}. The limiting wall value of the turbulent time scale $(\overline{q^2}/y^{+2}\epsilon^+)$ is equal to 1. It follows that $(-\overline{u^+v^+}\ \partial\overline{U}^+/\partial y^+)/(y^{+3}\epsilon^+)$, which is the limiting wall value of the ratio of turbulent energy production to turbulent energy dissipation is also unchanged.

Table II shows that there are important increases in the wall values of the skewness of $\partial u/\partial x$ ($S_{\partial u/\partial x} = \overline{(\partial u/\partial x)^3}/\overline{(\partial u/\partial x)^2}^{\frac{3}{2}}$) and the skewness of $\partial p/\partial x$. The large changes in $S_{\partial p/\partial y}$ and $S_{\partial p/\partial z}$ are spurious, the former quantity exhibiting relatively large scatter near the wall while the latter should strictly be zero by virtue of symmetry with respect to the $x-y$ plane. The increase in $S_{\partial u/\partial x}$ may reflect an increase in vorticity production even though the equality between the latter two quantities is strictly valid for isotropic turbulence.

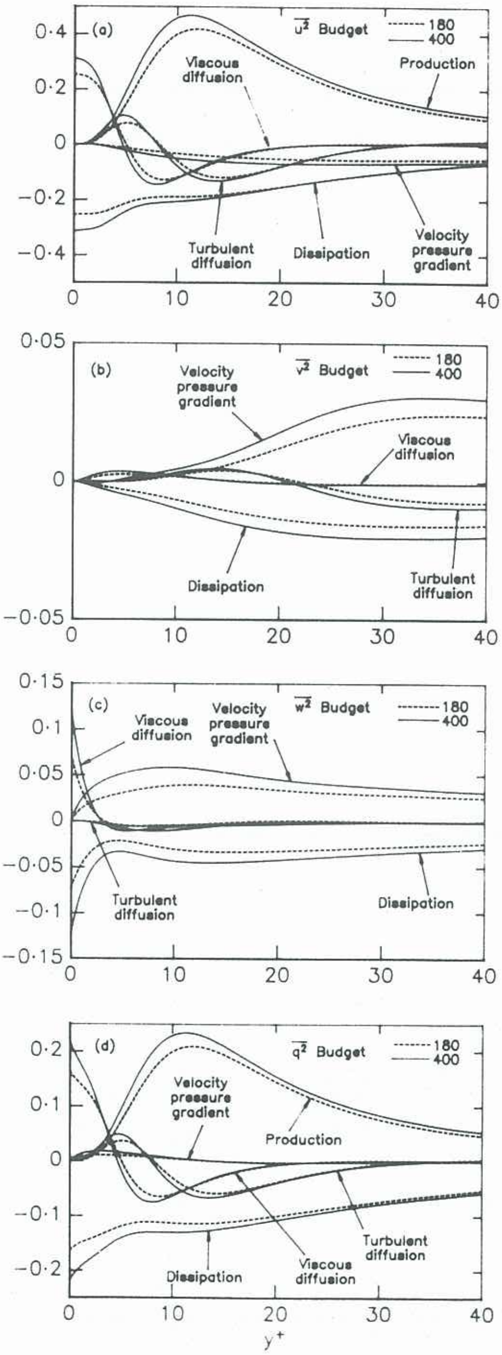

Figure 1 Budget of the Reynolds normal stresses and of their sum in wall region.

Table II : Effect of Reynolds Number on the Skewnesses of u, p and their Derivatives at the Wall

Quantity	$h^+ = 180$	$h^+ = 395$	Percentage Increase
S_u	0.836	0.95	14
$S_{\partial u/\partial x}$	-0.125	-0.224	79
$S_{\partial u/\partial y}$	0.838	0.952	14
$S_{\partial u/\partial z}$	-5.1×10^{-2}	-4.57×10^{-2}	-10
S_p	-0.109	-9.37×10^{-2}	14
$S_{\partial p/\partial x}$	0.327	0.867	165
$S_{\partial p/\partial y}$	0.737*	1.255*	70*
$S_{\partial p/\partial z}$	8.123×10^{-2}*	-5.44×10^{-2}*	-167*

*These values may be relatively inaccurate.

NEAR-WALL REGION

The DNS distributions of the Reynolds stresses have been presented in Antonia et al. (1992) and compared with measurements in the same flow. The dependence on h^+ of $-\overline{u^+v^+}$ and v'^+ in the wall region ($y^+ \lesssim 40$) strongly pointed to the active motion being Reynolds number dependent. This dependence would be consistent with Wei and Willmarth's (1989) speculation that associated with an increase in h^+ is an increased stretching of the vortices, beyond that required for scaling on wall variables. Direct support for the latter speculation was provided by the observed increases in $\omega_x'^+$ and $\omega_z'^+$ (Antonia et al., 1991; see also the following Section). Accompanying these increases is an increase in the turbulent energy dissipation ϵ (the homogeneous relation $\epsilon = \nu\overline{\omega^2}$ is closely approximated). The way the increase in ϵ is apportioned among the three Reynolds normal stresses can be ascertained from Figure 1 which shows the distributions of all the terms in the transport equations for $\overline{u^2}$, $\overline{v^2}$, $\overline{w^2}$ and of their sum $\overline{q^2}$. Clearly, the increase in the dissipation of $\overline{u^2}$ is confined mainly below $y^+ = 10$ while the percentage increases in the dissipation of $\overline{v^2}$ and $\overline{w^2}$ are important throughout the wall region. Note that the latter increases are balanced by corresponding increases in the production terms (velocity-pressure gradient correlations in the case of $\overline{v^2}$ and $\overline{w^2}$). The h^+ dependence of the two types of diffusion terms is generally small except in the case of the viscous diffusion which must balance the dissipation at the wall.

STREAMWISE VORTICES IN NEAR-WALL REGION

Kim et al. (1987) explained their distribution of $\omega_x'^+$ (at $h^+ = 180$) in terms of a (simplified) flow module comprising single streamwise Rankine vortices. The average position y_c^+ of the vortex centre was assumed to be equal to 20 (where $\omega_x'^+$ has a local maximum $\omega_{xc}'^+$) while the average vortex radius was taken to be equal to 15 wall units ($\omega_x'^+$ has a local minimum at $y_e^+ \simeq 5$). With such a model, it can be shown that (Kim et al., 1987)

$$\frac{\omega_{xc}'^{\,+}}{\omega_{xw}'^{\,+}} = 2\frac{y_e^+}{(y_c^+ - y_e^+)} \qquad (13)$$

where $\omega_{xw}'^{\,+}$ is the value of $\omega_x'^+$ at $y^+ = 0$. For the values of y_c^+ and y_e^+ assumed by Kim et al. (1987), the ratio is equal to 0.67. The present data for $\omega_x'^+$ (Figure 2) corroborate the selected values of y_c^+ and y_e^+ reasonably well. The ratio is equal to 0.74 for $h^+ = 180$ and 0.71 for $h^+ = 400$. These values are in reasonable agreement with Eq. (13) [note a decrease in y_c^+ between 20 to 19 — which is within the uncertainty of estimating the location of the local maximum — would increase the ratio from 0.67 to 0.71].

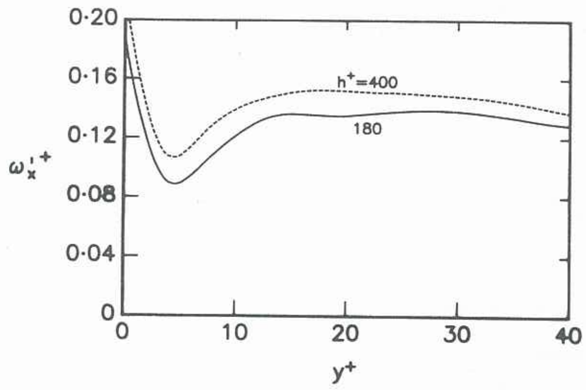

Figure 2 Root mean square streamwise vorticity in wall region.

The above considerations suggest that the dependence of ω_{xw}' on h^+ may be explained in terms of increase in strength of the vortex, without any significant change to its size. Figure 3 shows that the correlation coefficient $\overline{\omega_x(y)\omega_x(y+\Delta y)}/\omega_x'(y)\omega_x'(y+\Delta y)$ at $y^+ = 15$ is virtually unaffected by h^+ (the distance between the zero crossing points may be interpreted as a measure of the average vortex size). The rather large negative value of the coefficient near the wall (at $\Delta y^+ = -15$) reflects the presence of vorticity of opposite sign to that of the overlying vortex which results from the no-slip condition at the wall. The correlation coefficient $\overline{\omega_y(y)\omega_y(y+\Delta y)}/\omega_y'(y)\omega_y'(y+\Delta y)$ at $y^+ = 15$ is unaffected by h^+. This, in addition to our earlier comments on $\omega_y'^+$, suggests that both the scale and the strength of ω_y seem unaffected by h^+.

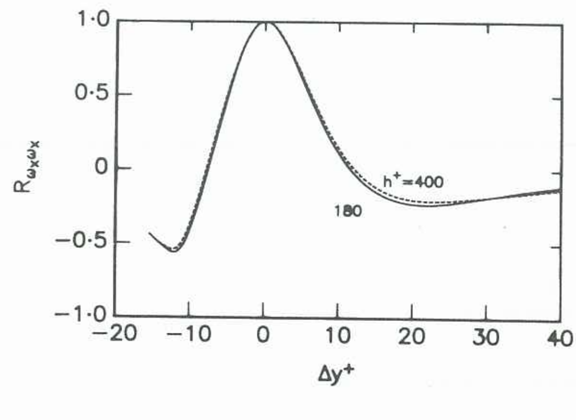

Figure 3 Two-point streamwise vorticity correlation coefficient as a function of Δy^+. The reference location is at $y^+ = 15$.

There is adequate support for the existence and importance of streamwise vortices near the wall, although not necessarily in the form of counter-rotating vortex pairs with spanwise separation. Robinson (1990) has computed several statistics for the locations, size and strength of streamwise and spanwise vortices using a DNS data base for the boundary layer. His results point to a clustering of quasi-streamwise vortices near the wall. The most probable values for the location and diameter of these vortices are very similar to the present suggestions.

The increased intensity of the vortices would lead to an increase in the magnitude of $\overline{u^+v^+}$. Ejection and sweep-like motions, which may occur on the upward and downward rotating sides of the streamwise vortices, are likely to be strengthened as is the so-called splatting motion (e.g. Moin and Kim, 1982; Chapman and Kuhn, 1986). The stronger splatting motions caused by the stronger streamwise vortices would also cause stronger spanwise vorticity fluctuations at the wall. Kim (1992) has shown that a key strategy for viscous drag reduction is to limit the interaction between streamwise vortices and the wall. It would appear that the Reynolds number effect acts directly on ω_x through the increased vortex stretching and, perhaps less directly through the increased splatting, on ω_z. The smaller increase at the wall of $\omega_z'^+$, compared with $\omega_x'^+$, would be consistent with this speculation.

It seems plausible that the increased vortex stretching would explain, at least qualitatively, the increase of, inter alia, the Reynolds normal stresses, shear stresses and energy dissipation. The increased vortex stretching is also consistent with the suggestion by Antonia et al. (1992) that the "active" motion is Reynolds number dependent. It is possible that the intensity of spanwise vortices is also increased as h^+ increases (distributions of $\omega_z'^+$ support this) but the statistics for the most probable locations, size and strength of these vortices (Robinson, 1990) suggests that their importance is likely to be felt towards the outer part of the wall layer.

CONCLUSIONS

The present results indicate that there are significant low Reynolds number effects in the near-wall region of a turbulent duct flow. These effects are consistent with the suggestion that quasi-streamwise vortices are intensified as the Reynolds number increases. Turbulence models for wall-bounded shear flows will need to account for these effects. The recent success by Durbin (1992), who directly computed the wall-normal component (v) and the corresponding velocity pressure-gradient term using $k - v - \epsilon$ equations in predicting several wall-bounded turbulent flows, is consistent with the above conclusion.

ACKNOWLEDGEMENT

RAA acknowledges the support of the Australian Research Council.

REFERENCES

ANTONIA, R. A., KIM, J. and BROWNE, L. W. B. (1991) Some Characteristics of Small-Scale Turbulence in a Turbulent Duct Flow. *J. Fluid Mech.*, **233**, 369-388.

ANTONIA, R. A., TEITEL, M., KIM, J. and BROWNE, L. W. B. (1992) Low Reynolds Number Effects in a Fully Developed Turbulent Channel Flow. *J. Fluid Mech.*, **236**, 579-605.

CHAPMAN, D. R. and KUHN, G. D. (1986) The Limiting Behaviour of Turbulence Near a Wall. *J. Fluid Mech.*, **170**, 265-292.

DURBIN, P. (1992) Application of a Near-Wall Turbulent Model to Boundary Layers and Heat Transfer, *CTR Manuscript 132*, Center for Turbulence Research, Stanford University, Stanford, CA.

HANJALIC, K. and LAUNDER, B. E. (1976) Contribution Towards a Reynolds-Stress Closure for Low-Reynolds-Number Turbulence. *J. Fluid Mech.*, **74**, 593-610.

KIM, J. (1992) Study of Turbulence Structure Through Numerical Simulations : The Perspective of Drag Reduction, in *AGARD Report (R-786)*, AGARD FDP/VKI Special Course on "Skin Friction Drag Reduction", 2-6 March 1992, VKI, Brussels, Belgium.

KIM, J. (1989) On the Structure of Pressure Fluctuations in Simulated Turbulent Channel Flow. *J. Fluid Mech.*, **205**, 421-451.

KIM, J., MOIN, P. and MOSER, R. (1987) Turbulence Statistics in Fully Developed Channel Flow at Low Reynolds Number. *J. Fluid Mech.*, **177**, 133-166.

MANSOUR, N. N. (1991) The Use of Direct Numerical Simulation Data in Turbulence Modeling. *Paper AIAA 91-0221.*

MANSOUR, N. N., KIM, J. and MOIN, P. (1988) Reynolds-Stress and Dissipation-Rate Budgets in a Turbulent Channel Flow. *J. Fluid Mech.*, **194**, 15-44.

MANSOUR, N. N., KIM, J. and MOIN, P. (1989) Near-Wall $k - \epsilon$ Turbulence Modeling. *AIAA Jnl.*, **27**, 1068-1073.

MOIN, P. and KIM, J. (1982) Numerical Investigation of Turbulent Channel Flow, *J. Fluid Mech.*, **118**, 341-377.

ROBINSON, S. K. (1990) A Review of Vortex Structures and Associated Coherent Motions in Turbulent Boundary Layers. In *Structure of Turbulence and Drag Reduction*, A. Gyr, ed., Springer, 23-50.

RODI, W. and MANSOUR, N. N. (1990) Low Reynolds Number $k - \epsilon$ Modeling with the Aid of Direct Simulation Data. *Proc. Summer Program*, Center for Turbulence Research, Stanford University, 85-106.

SO, R. M. C., LAI, Y. G., ZHANG, H. S. and HWANG, B. C. (1991a) Second-order Near-Wall Turbulence Closures : A Review. *AIAA Jnl.*, **29**, 1819-1835.

SO, R. M. C., ZHANG, H. S. and SPEZIALE, C. G. (1991b) Near-Wall Modelling of the Dissipation-Rate Equation. *AIAA Jnl.*, **29**, 2069-2076.

SPALART, P. R. (1988) Direct Simulation of a Turbulent Boundary Layer up to $R_\theta = 1410$. *J. Fluid Mech.*, **187**, 61-98.

TOWNSEND, A. A. (1956) *The Structure of Turbulent Shear Flow*, C.U.P.

WEI, T. and WILLMARTH, W. W. (1989) Reynolds Number Effects on the Structure of a Turbulent Channel Flow. *J. Fluid Mech.*, **204**, 57-95.